



Highly Flexible Fabric-Based Organic Light-Emitting Devices for Conformal Wearable Displays

Da Yin, Zhi-Yu Chen, Nai-Rong Jiang, Yue-Feng Liu, Yan-Gang Bi, Xu-Lin Zhang, Wei Han, Jing Feng,* and Hong-Bo Sun*

Organic light-emitting devices on fabrics (Fa-OLEDs) are outstanding candidates for high-quality wearable displays. High flexibility and conformality to clothes deformations are required for Fa-OLEDs to keep wearing comfort during body movement. However, it is a great challenge to realize an ultrathin planarization layer with ultrasmooth surface simultaneously on the rough surface of fabrics for Fa-OLEDs fabrication. Here, a template-stripping process is employed to fabricate both ultrathin and ultrasmooth planarization layers for highly flexible and efficient Fa-OLEDs. The thickness of the planarization layer is as small as 3 μm while its surface roughness is only 0.6 nm. The planarization process is insensitive to the textures and morphology of fabrics. As a result, the Fa-OLEDs show excellent electroluminescent performance and flexibility. The maximum current efficiency of 78 cd A^{-1} is comparable with that of the conventional planar devices. The variation of current efficiency is as small as 8% after 1000 times of bending with 1 mm bending radius, which is the best bending stability of the flexible Fa-OLEDs reported to date. The Fa-OLEDs are successfully used as conformal wearable displays by sewing on clothes and keep working well with a series of arm movements.

Fabric-based electronic devices have been widely researched due to their great application potential in wearable equipment in recent years. A number of optoelectronic functions, such as sensing, triboelectric power-generation, solar energy conversion, and energy storage, have been integrated into fabrics to form smart clothing.^[1–8] Light-emitting devices fabricated on fabrics (Fa-LEDs) are essential for realizing wearable displays and have attracted much attention.^[9] In order to keep wearing comfort, Fa-LEDs have to possess high flexibility and conformality to accommodate the clothes deformations during body movement. Flexible fiber-shaped LEDs have been reported^[10–18] and dynamic and static fabric displays based on the light-emitting fibers have been demonstrated by Zhang and coworkers successfully.^[14] However, an abnormal and complicated fabrication process and the difficulties in the integration of thin film transistors on the fibers restrict their

applications for active matrix driving displays. Another strategy is fabricating planar LEDs on fabric substrates for flat panel displays. However, fabrics usually have porous and rough surfaces which are not suitable for fabricating planar devices. Polymer planarization layers have been used to improve the surface appearance of fabrics. Flexible Fa-LEDs with electroluminescent (EL) phosphor particles as emitting materials on polymer planarization layers have been researched.^[19,20] These devices are driven with alternating current at high voltage while have a low luminance and efficiency, which is not compatible with the demands of wearable displays for portable applications.

Organic light-emitting devices (OLEDs) with flat structure possess advantages of high flexibility, high efficiency, low driving voltage, and light weight^[12,21–25] and exhibit great potential in fabric-based wearable displays. The total thickness of an OLED, including electrodes, hole and electron transporting layers, and emitting layers, is about 100–200 nm. Highly smooth substrate is crucial for the high efficiency and long-term stability of the OLEDs. In order to achieve high performance of Fa-OLEDs, the planarization layers are required to smoothen the surface of the fabrics to avoid deficient interface contact and leakage current.^[24,26] However, the surface profile of the planarization layer is prone to duplicate the morphology of the rough fabrics, so that a very thick layer is needed to fully

Dr. D. Yin, Z.-Y. Chen, N.-R. Jiang, Dr. Y.-F. Liu, Dr. Y.-G. Bi, Dr. X.-L. Zhang, Prof. J. Feng
State Key Laboratory of Integrated Optoelectronics
College of Electronic Science and Engineering
Jilin University
2699 Qianjin Street, Changchun 130012, China
E-mail: jingfeng@jlu.edu.cn

Prof. W. Han
Sino-Russian International Joint Laboratory for Clean Energy and Energy Conversion Technology
College of Physics
Jilin University
Changchun 130012, China

Prof. W. Han
International Center of Future Science
Jilin University
Changchun 130012, China

Prof. H.-B. Sun
State Key Laboratory of Precision Measurement Technology and Instruments
Department of Precision Instrument
Tsinghua University
Haidian, Beijing 100084, China
E-mail: hbsun@tsinghua.edu.cn

The ORCID identification number(s) for the author(s) of this article can be found under <https://doi.org/10.1002/admt.201900942>.

DOI: 10.1002/admt.201900942

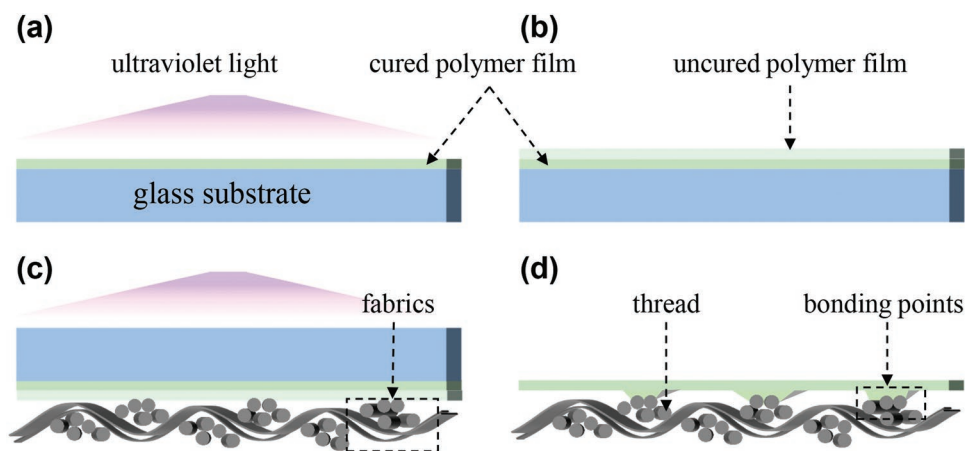


Figure 1. Schematic diagram of the fabric planarization by using the template-stripping process. a) Spin-coating a photosensitive polymer film on a flat glass substrate followed by UV light curing. b) Spin-coating another photosensitive polymer film on the cured polymer film. c) Covering the polymer/glass substrate on the surface of the fabrics with the polymer film facing down followed by UV curing again. The first polymer film is used as the planarization layer and the second polymer film is used as a bonding layer between the fabrics and the planarization layer. d) Peeling off the glass substrate and leaving the polymer film on the surface of the fabrics. A flat and smooth surface for the fabrics is formed.

cover the fabrics and obtain a smooth surface. Spin-coating or laminating polymer films with their thickness larger than 30 μm on the surface of fabrics has been used to fabricate Fa-OLEDs.^[27–32] Although high efficiency of about 70 cd A^{-1} has been achieved, the flexibility of these devices is restricted by the 100 μm -thick planarization layers.^[28] Large bending strain results in faint cracks and efficiency degradation when the device is bent to 2 mm radius. When the device is bent to 1 mm bending radius, fatal cracks are formed and result in an electrical short circuit and device failure. On this occasion, no electrical and optical characteristics are measurable. It is a great challenge to realize an ultrathin planarization layer with ultrasmooth surface simultaneously on the rough surface of fabrics for highly flexible and efficient Fa-OLEDs fabrication.

Here, we employ a simple template-stripping process to transfer an ultrathin planarization film with ultrasmooth surface to the fabrics for highly flexible and efficient Fa-OLEDs. The thickness of the planarization film can be much decreased to only 3 μm by using this process while its surface roughness is only 0.6 nm. The planarization film consists of a bi-layer structure in which one layer is used to provide a flat and smooth surface and the other layer is used to provide an interfacial bonding strength between the fabrics and the planarization film. It is a universal method to planarize fabrics with various materials and weaving structures by using ordinary polymers, for example, commercial adhesives. As a result, excellent EL performance and flexibility have been obtained for the Fa-OLEDs. The maximum current efficiency of 78 cd A^{-1} is comparable with that of the conventional planar devices. The variation of current efficiency is as small as 8% after 1000 times of bending with 1 mm bending radius, which is the best bending stability of Fa-OLEDs reported to date. More importantly, the Fa-OLEDs work well under various bending deformation along with arm movement when sewed on clothes. This work promotes the development of conformal wearable displays based on the Fa-OLEDs.

Figure 1 exhibits the procedure of the fabric planarization by using the template-stripping process. A photosensitive polymer

is spin-coated on a flat glass substrate and cured by ultraviolet (UV) light (Figure 1a). Then the same photosensitive polymer is spin-coated again on the cured polymer layer (Figure 1b). The polymer/glass substrate is transferred to the surface of the fabrics with the polymer film facing down (Figure 1c). The second polymer is cured by UV exposure. The first polymer film acts as the planarization layer and the second polymer film acts as a bonding layer between the planarization layer and the fabrics. Finally, the fabric together with the planarization film is peeled off from the glass substrate (Figure 1d). The interface characteristics between the two photosensitive layers are important for the template-stripping process. Figure S1, Supporting Information, shows the cross-sectional scanning electron microscope (SEM) image of a bi-layer-structure polymer film composed of the photosensitive polymer. No obvious interface can be observed. Additionally, the two layers cannot be separated by bending or twisting the film. This means that the adhesion between the two layers is strong.

Figure 2a–f shows the SEM images of six kinds of fabrics with different materials and surface appearance, including nylon, cotton, linen, silk, polyester, and terylene, which are half covered by planarization layers. It can be seen that all the planarization layers on different fabrics are smooth. The planarization layer is only about 3 μm thick and very transparent, which is beneficial for the latter curing process of the second photosensitive polymer film. Its transmittance is about 85–89% in the range of 350–380 nm (Figure 2g). The photosensitive polymer has the maximum absorption in this wavelength range and could be cured by UV light easily.

It can be seen from the SEM images that the thickness and appearance of the planarization layers are insensitive to the textures and morphology of various fabrics. This is due to the smooth surface of the glass substrate, which acts as a template in the template-stripping process. The glass substrate is very smooth with its surface roughness of 0.4 nm obtained from the atomic force microscope (AFM) (Figure 2h). The surface of the planarization layer contacted to the glass substrate duplicates the surface morphology of the glass, and keeps smooth

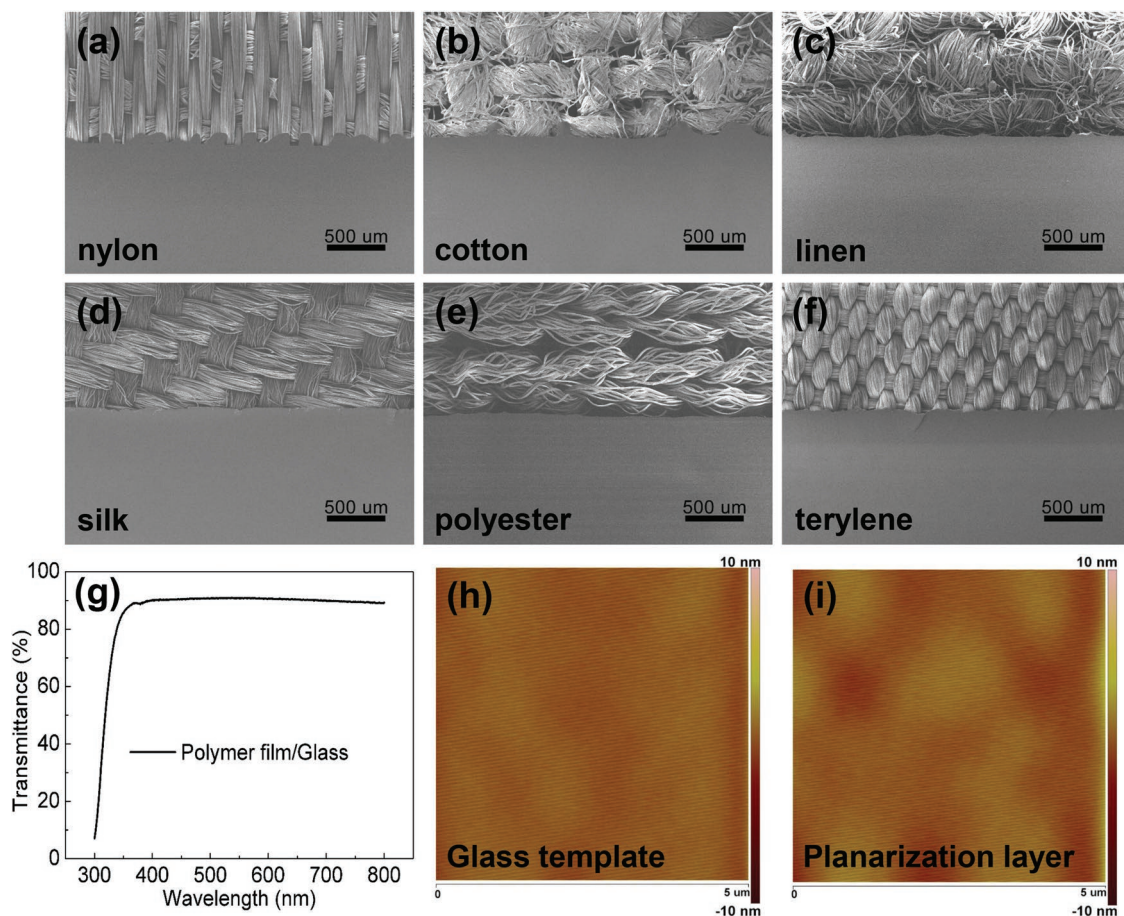


Figure 2. SEM images of six kinds of fabrics half covered with planarization layers: a) nylon, b) cotton, c) linen, d) silk, e) polyester, f) terylene. g) Transmittance spectra of cured polymer film/glass substrate. h) AFM image of the surface of a glass substrate. i) AFM image of the surface of a planarization layer on fabrics.

after peeled off from the glass substrate (Figure 1d). Its surface roughness is only 0.6 nm on various fabrics (Figure 2i) which is five orders of magnitude smaller than that of the rough fabrics. The template-stripping process described here has successfully decreased the dependence of the planarization layer morphology on the surface profile of the various fabrics, which provides ultrathin and smooth planarization layers for efficient and flexible Fa-OLEDs.

The planarization effect of the template-stripping process compared to that by the direct spin-coating on nylon (nylon is neat and weaved tidily without unnecessary thread residues and suitable for spin-coating) is investigated in detail and shown in Figure 3. The planarization layer fabricated by template-stripping process is able to cover the rough surface of the fabric while keeping flat. The thickness of the planarization layer is uniform as can be seen in Figure 3a. There is interspace between the fabric and the planarization layer. The polymer penetrates little into the fabric and stays at the bonding points as shown in the enlarged cross-sectional SEM image (Figure 3b). It means that they are bonded together at the raised thread regions of the fabric. This is beneficial to maintaining its flexibility and guaranteeing the bonding strength between the fabric and planarization film. As a contrast, the weaving structure of the

nylon can be seen clearly when the polymer is spin-coated directly on the nylon surface with the same parameter used in the template-stripping process (Figure 3c). This is because lots of the polymer penetrates into the fabric and the remaining part on the surface is not able to fully fill in the surface structure and tends to duplicate the surface profile of the fabric. This is demonstrated by the cross-sectional SEM image as shown in Figure 3d. The thread is bonded together by the penetrated photosensitive polymer. The rough surface is not suitable for OLED fabrication. Smooth spin-coated planarization layer can be achieved by increasing thickness of the polymer film, while the flexibility would decrease considerably.^[27]

It can be concluded from the above comparison that the template-stripping process has obvious advantages over spin-coating in ultrathin and smooth planarization layer fabrication. Fa-OLED is fabricated on nylon with the template-stripped planarization layer. Orange-emitting phosphorescent materials Ir(BT)2(acac) (Bis(2-phenyl-benzothiazole-C2,N) (acetylacetonate)iridium(III)) is used as emitter. A conventional planar OLED fabricated on the silicon substrate is also fabricated for comparison. The EL performance of the Fa-OLEDs is comparable to that of the conventional OLED as can be seen in Figure 4. The device is turned on at 3.5 V. The maximum

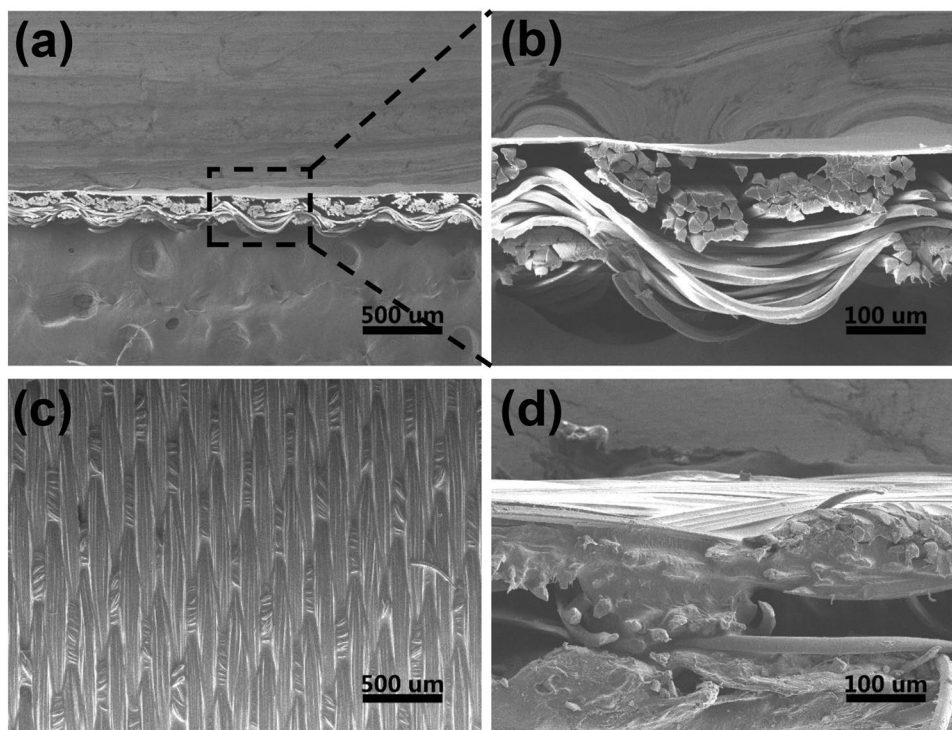


Figure 3. a) Cross-sectional SEM image and b) enlarged image of nylon planarized by the template-stripping process. c) Top-view and d) cross-sectional SEM images of nylon planarized by direct spin-coating of a polymer film.

luminance and current efficiency are $15\,000\text{ cd m}^{-2}$ and 78 cd A^{-1} , respectively. The excellent EL performance is attributed to the flat and smooth planarization layer, which is crucial for the highly efficient Fa-OLEDs.

Fa-OLEDs fabricated on other kinds of fabrics are shown in Figure S2, Supporting Information. All devices show uniform light emission, which demonstrates the planarization effect of the polymer films. However, it should be noted that the efficiency of the devices is influenced by the surface appearance of the fabrics. Compared to nylon, linen has a rougher surface with lots of thread residues (Figure 2c). We compared the EL performance of OLEDs on nylon, linen, and conventional silicon substrates (Figure S3, Supporting Information). The OLEDs on linen have the largest leakage current and lowest luminance,

which results in the lowest current efficiency. Although the surface of the planarization layer on linen is smooth, the ultrathin planarization layer is not as flat as the glass template due to the rough surface of linen with residues and large weaving structures, which results in the large leakage current.

High flexibility is expectable for the Fa-OLED with the ultrathin planarization layer. Figure 5a,b shows the photographs of the Fa-OLEDs on nylon under a bending radius of 2 mm. Uniform emission across the whole emitting area is observed, and the device exhibits outstanding bending stability. A cyclic bending test is conducted at the 2 mm bending radius (Figure 5c). The values of current density and luminance fluctuate almost synchronously. The degradations are only about 0.2% and 1.7%, respectively after 1000 bending cycles. Notably, the degradation

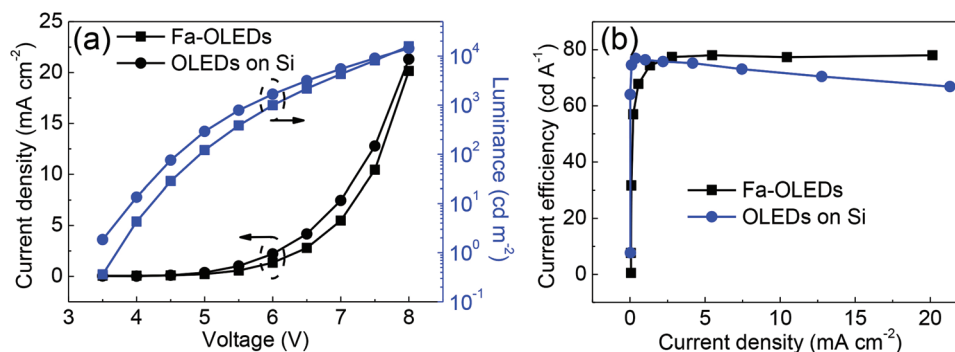


Figure 4. Electroluminescent performance of the Fa-OLEDs. a) Luminance and current density curves of the Fa-OLEDs with increased driving voltage. b) Current efficiency curve of the Fa-OLEDs with increased current density. The EL performance of conventional OLEDs on a Si substrate is plotted for comparison.

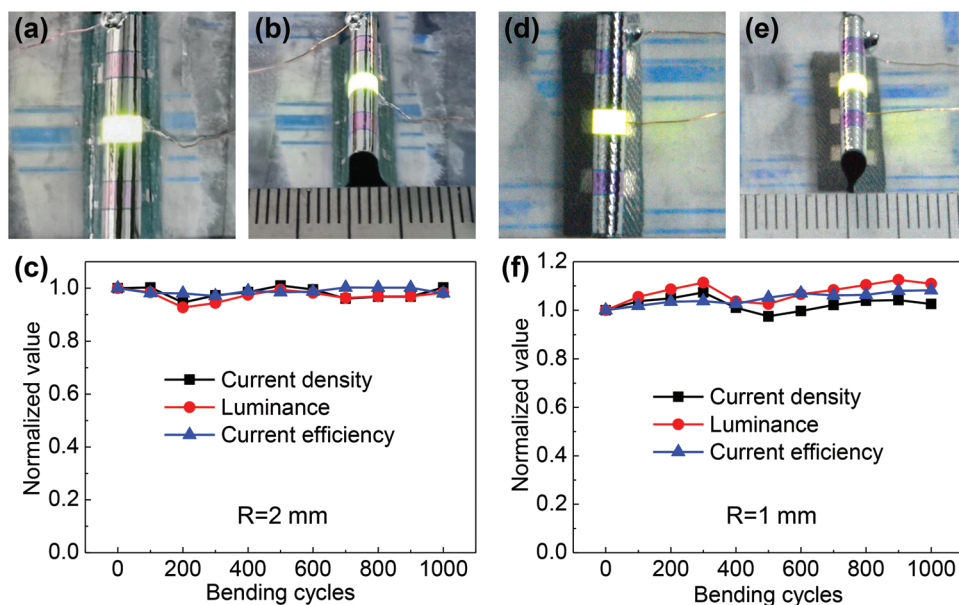


Figure 5. Mechanical stability of the Fa-OLEDs. a) Top view and b) front view of the operating Fa-OLEDs with 2 mm bending radius. The size of the emission region is 1.5 mm × 5 mm. c) Normalized values of current density, luminance, and current efficiency curves of the Fa-OLEDs under 1000 bending cycles with 2 mm bending radius. d) Top view and e) front view of the operating Fa-OLEDs with 1 mm bending radius. The size of the emission region is 2 mm × 5 mm. f) Normalized values of current density, luminance, and current efficiency curves of the Fa-OLEDs under 1000 bending cycles with 1 mm bending radius.

of current efficiency is as small as 2%. The bending radius is further decreased to 1 mm for the Fa-OLEDs (Figure 5d,e). Bright emission is observed without any dark dots, lines, or electrical short which are usually caused by large bending stress-induced cracks in the device.^[28] More importantly, the variation of current efficiency is as small as 8% after 1000 bending cycles at 1 mm bending radius as seen in Figure 5f, which is the best bending stability of Fa-OLEDs reported to date. The bending strain of a thin film can be calculated by a simplified equation

$$\varepsilon = \frac{T}{2R} \quad (1)$$

where ε is the bending strain, T represents the thickness of the planarization layer, and R represents the bending radius. The variation of the EL performance at 1 mm bending radius is mainly due to the bending strain of the Fa-OLEDs with the small bending radius. The bending strain of the Fa-OLEDs with the 3 μm planarization layer is about 0.15% according to Equation (1). The metal electrodes of the Fa-OLEDs have a much higher strain threshold of about 1–2%, therefore the bending deformation does not deteriorate the Fa-OLEDs.^[33]

The lifetime of the Fa-OLED is measured by continuously driving the device at a constant voltage model as shown in Figure S4, Supporting Information. It can be seen that the luminance and current efficiency decrease with time increasing. The current density increases rapidly and irregularly after 200 min. However, the luminance does not increase with the current density. As a result, the current efficiency drops fast due to the large leakage current. The dark dots at the surface of light-emitting area can be observed obviously after 240 min (Inset in Figure S4, Supporting Information). The low

air relative humidity (18%) of the testing environment is beneficial for the lifetime and the stable EL performance during cyclic bending test of the Fa-OLED.

The highly flexible Fa-OLEDs have inherent advantages in applications of conformal wearable displays. They can be easily integrated into clothing and deform with body movement while maintaining wearing comfort. Here the Fa-OLED is sewed on clothes as a demonstration (Figure 6a–d). The Fa-OLEDs are highly conformal to clothes during arm moving (Movie S1, Supporting Information). It works well under a series of deformations, even when poked by the elbow or wrinkled by the bending arm. Furthermore, a series of patterned Fa-OLEDs is fabricated and integrated on clothes as light-emitting label (Figure 6e–h). These results demonstrate that the Fa-OLEDs have great potential in wearable electronics.

We report highly flexible and conformal Fa-OLEDs by using the simple and universal template-stripping process to planarize the surface of the fabrics with various materials and weaving structures. The current efficiency of the Fa-OLED reaches up to 78 cd A^{-1} and keeps fairly stable with 8% variation after 1000 times of bending cycles with 1 mm bending radius. The high efficiency and flexibility of the Fa-OLEDs offer great potential for their applications in conformal wearable displays. It could keep working under a series of deformations by sewing on clothes. We expect that the Fa-OLEDs reported here can provide a possible opportunity for large-area and high-quality wearable displays. However, it should be noted that the thickness of the planarization layer is only 3 μm which makes it short of mechanical reliability, such as blocking violent external mechanical intrusions or friction. Additionally, optimizations of the fabrication process of Fa-OLEDs are necessary to integrate them with transistors by using the conventional semiconductor

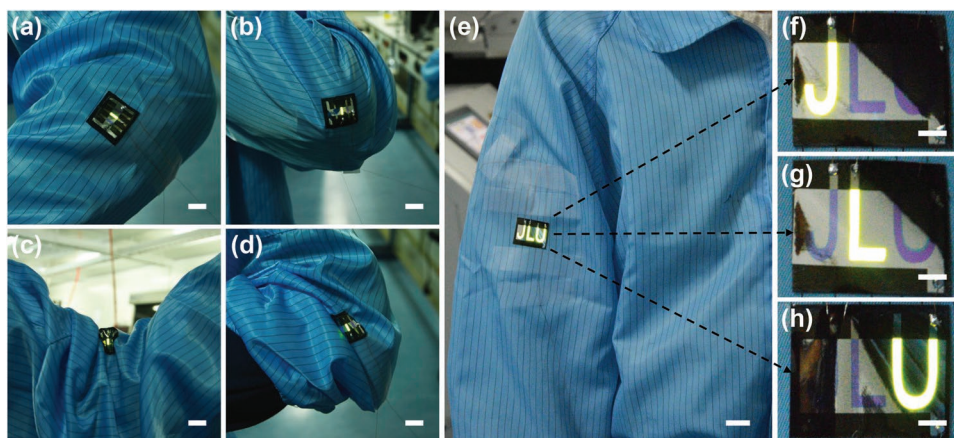


Figure 6. Photographs of Fa-OLEDs fixed on clothes. a–d) Fa-OLEDs are sewn on clothes and deformed with arm moving. They keep working well with a series of arm movements. The size of OLED is 1.5 mm × 5 mm. Scale bar is 10 mm. e) Fa-OLEDs work as wearable displays. JLU is short for Jilin University. The scale bar is 20 mm. f–h) Enlarged images of J, L, U light-emitting units. Scale bar is 5 mm.

technology for active matrix driving wearable displays. So, more research efforts are needed to make the Fa-OLEDs on the way toward real applications.

Experimental Section

Planarization Layers Fabrication: Fabrics were purchased from shops and used as received. They were cut into rectangles with size of 3 cm × 5 cm and bonded on glass sheets by tapes. NOA 63 photosensitive polymer made by Norland Products, Inc. was first diluted by acetone at a ratio of 1:1 by mass. Then it was spin-coated on a clean glass substrate at 8000 rpm for 60 s. The film thickness was about 3 μm after UV light curing. Then the polymer was spin-coated again on the cured film under the same parameters. The glass substrate was coated on the previously prepared fabrics with the polymer layer facing down. The second NOA 63 layer was used as glue for bonding the first polymer film and the fabrics together. Finally, the polymer film/fabric was peeled off from the glass substrate together after the second UV curing. The first polymer film left on the fabric surface was used as a planarization layer.

Fa-OLEDs Fabrication: OLED was fabricated on the surface of the planarization layer by vacuum thermal evaporation. Its structure was composed of organic functional layers sandwiched between two metal electrodes, where 80 nm Ag was the anode, 3 nm MoO₃ was the hole injection layer, NPB (*N,N'*-diphenyl-*N,N'*-bis(1,1'-biphenyl)-4,4'-diamine) (40 nm) was the hole transport layer, CBP (4,4'-Bis(9*H*-carbazol-9-yl)-biphenyl) (30 nm) was the host material, Ir(bt)₂(acac) (Bis(2-phenylbenzothiazole-C₂,*N*)(acetylacetonate)iridium(III)) (5% doped in CBP) was the guest material, TPBi (1,3,5-Tris(1-phenyl-1*H*-benzimidazol-2-yl)-benzene) (30 nm) was the electron transport layer, Ca (3 nm) was the electron injection layer, and Ag (18 nm) was the cathode. The metals were supplied by ZhongNuo Advanced Material Technology Co., Ltd. MoO₃ and other organic materials were supplied by Xi'an Polymer Light Technology Corp. The planar OLEDs on Si substrates were fabricated with the same device structure and materials.

Characterizations: JEOL JSM-7500F was put to use for SEM images. Dimension Icon XP-2 stylus profilometer (Ambios Technology, Inc.) was put to use for film thickness measurement. AFM (Bruker Corporation) was put to use for AFM images. The EL characteristics of Fa-OLEDs were measured by a source meter (Keithley 2400) and a spectrophotometer (Photoresearch 655). Fa-OLEDs bending test was conducted on a home-made stage. All OLEDs were measured in the air without encapsulation. The temperature and the air relative humidity of the test room were about 20 °C and 18%, respectively, which were modulated by an air conditioner.

Supporting Information

Supporting Information is available from the Wiley Online Library or from the author.

Acknowledgements

This work was supported by the National Key Research and Development Program of China and National Natural Science Foundation of China (NSFC) under Grants #2017YFB0404500, #61805096, #61825402, #61675085, and 61705075 and also supported by the China Postdoctoral Science Foundation under Grant 2019M651201.

Conflict of Interest

The authors declare no conflict of interest.

Keywords

fabrics, organic light-emitting devices, ultrathin planarization layers, wearable displays

Received: October 20, 2019

Revised: December 28, 2019

Published online:

- [1] S. K. Sinha, Y. Noh, N. Reljin, G. M. Treich, S. Hajeb-Mohammadali pour, Y. Guo, K. H. Chon, G. A. Sotzing, *ACS Appl. Mater. Interfaces* **2017**, *9*, 37524.
- [2] Y. Li, Y. Li, M. Su, W. Li, Y. Li, H. Li, X. Qian, X. Zhang, F. Li, Y. Song, *Adv. Electron. Mater.* **2017**, *3*, 1700253.
- [3] S. S. Kwak, H. Kim, W. Seung, J. Kim, R. Hinchet, S. W. Kim, *ACS Nano* **2017**, *11*, 10733.
- [4] E. Bihar, T. Roberts, E. Ismailova, M. Saadaoui, M. Isik, A. Sanchez-Sanchez, D. Mecerreyes, T. Hervé, J. B. De Graaf, G. G. Malliaras, *Adv. Mater. Technol.* **2017**, *2*, 1600251.
- [5] X. Pu, L. Li, M. Liu, C. Jiang, C. Du, Z. Zhao, W. Hu, Z. L. Wang, *Adv. Mater.* **2016**, *28*, 98.
- [6] J. Chen, Y. Huang, N. Zhang, H. Zou, R. Liu, C. Tao, X. Fan, Z. L. Wang, *Nat. Energy* **2016**, *1*, 16138.

- [7] Y. Huang, H. Hu, Y. Huang, M. Zhu, W. Meng, C. Liu, Z. Pei, C. Hao, Z. Wang, C. Zhi, *ACS Nano* **2015**, *9*, 4766.
- [8] W. Seung, M. K. Gupta, K. Y. Lee, K.-S. Shin, J.-H. Lee, T. Y. Kim, S. Kim, J. Lin, J. H. Kim, S.-W. Kim, *ACS Nano* **2015**, *9*, 3501.
- [9] J. S. Heo, J. Eom, Y. H. Kim, S. K. Park, *Small* **2018**, *14*, 1703034.
- [10] S. Kwon, W. Kim, H. Kim, S. Choi, B.-C. Park, S.-H. Kang, K. C. Choi, *Adv. Electron. Mater.* **2015**, *1*, 1500103.
- [11] B. O'Connor, K. H. An, Y. Zhao, K. P. Pipe, M. Shtein, *Adv. Mater.* **2007**, *19*, 3897.
- [12] Z. Zhang, L. Cui, X. Shi, X. Tian, D. Wang, C. Gu, E. Chen, X. Cheng, Y. Xu, Y. Hu, J. Zhang, L. Zhou, H. H. Fong, P. Ma, G. Jiang, X. Sun, B. Zhang, H. Peng, *Adv. Mater.* **2018**, *30*, 1800323.
- [13] S. Kwon, H. Kim, S. Choi, E. G. Jeong, D. Kim, S. Lee, H. S. Lee, Y. C. Seo, K. C. Choi, *Nano Lett.* **2018**, *18*, 347.
- [14] Z. Zhang, K. Guo, Y. Li, X. Li, G. Guan, H. Li, Y. Luo, F. Zhao, Q. Zhang, B. Wei, Q. Pei, H. Peng, *Nat. Photonics* **2015**, *9*, 233.
- [15] J. Y. Shih, S. L. Lai, H. T. Cheng, *Adv. Mater. Res.* **2013**, *821-822*, 453.
- [16] C. Zysset, N. Münzenrieder, T. Kinkeldei, K. Cherenack, G. Tröster, *IEEE Trans. Electron Devices* **2012**, *59*, 721.
- [17] M. Rein, V. D. Favrod, C. Hou, T. Khudiyev, A. Stolyarov, J. Cox, C. C. Chung, C. Chhav, M. Ellis, J. Joannopoulos, Y. Fink, *Nature* **2018**, *560*, 214.
- [18] K. J. Ko, H. B. Lee, H. M. Kim, G. J. Lee, S. R. Shin, N. Kumar, Y. M. Song, J. W. Kang, *Nanoscale* **2018**, *10*, 16184.
- [19] M. de Vos, R. Torah, M. Glanc-Gostkiewicz, J. Tudor, *J. Disp. Technol.* **2016**, *12*, 1757.
- [20] Y. Wu, S. S. Mechael, Y. Chen, T. B. Carmichael, *Adv. Mater. Technol.* **2018**, *3*, 1700292.
- [21] D. Yin, N. R. Jiang, Z. Y. Chen, Y. F. Liu, Y. G. Bi, X. L. Zhang, J. Feng, H. B. Sun, *Adv. Opt. Mater.* **2019**, 1901525.
- [22] B. Q. Liu, L. Wang, D. Y. Gao, J. H. Zou, H. L. Ning, J. B. Peng, Y. Cao, *Light: Sci. Appl.* **2016**, *5*, e16137.
- [23] R. Ding, X. P. Wang, J. Feng, X. B. Li, F. X. Dong, W. Q. Tian, J. R. Du, H. H. Fang, H. Y. Wang, T. Yamao, S. Hotta, H. B. Sun, *Adv. Mater.* **2018**, *30*, 1801078.
- [24] D. Yin, J. Feng, R. Ma, Y. F. Liu, Y. L. Zhang, X. L. Zhang, Y. G. Bi, Q. D. Chen, H. B. Sun, *Nat. Commun.* **2016**, *7*, 11573.
- [25] J. Xu, Y. Cui, G. M. Smith, P. Li, C. Dun, L. Shao, Y. Guo, H. Wang, Y. Chen, D. L. Carroll, *Light: Sci. Appl.* **2018**, *7*, 46.
- [26] Y.-F. Liu, J. Feng, D. Yin, Y.-G. Bi, J.-F. Song, Q.-D. Chen, H.-B. Sun, *Opt. Lett.* **2012**, *37*, 1796.
- [27] Y.-F. Liu, M.-H. An, Y.-G. Bi, D. Yin, J. Feng, H.-B. Sun, *IEEE Photonics J.* **2017**, *9*, 7000606.
- [28] S. Choi, S. Kwon, H. Kim, W. Kim, J. H. Kwon, M. S. Lim, H. S. Lee, K. C. Choi, *Sci. Rep.* **2017**, *7*, 6424.
- [29] W. Kim, S. Kwon, Y. C. Han, E. Kim, K. C. Choi, S.-H. Kang, B.-C. Park, *Adv. Electron. Mater.* **2016**, *2*, 1600220.
- [30] J. S. Kim, C. K. Song, *Org. Electron.* **2016**, *30*, 45.
- [31] H. Kim, S. Kwon, S. Choi, K. C. Choi, *J. Inf. Disp.* **2015**, *16*, 179.
- [32] W. Kim, S. Kwon, S.-M. Lee, J. Y. Kim, Y. Han, E. Kim, K. C. Choi, S. Park, B.-C. Park, *Org. Electron.* **2013**, *14*, 3007.
- [33] H. Huang, F. Spaepen, *Acta Mater.* **2000**, *48*, 3261.